

Optimization of Divergent Angle of a Rocket Engine Nozzle Using Computational Fluid Dynamics

¹Biju Kuttan P, ²M Sajesh

^{1,2}Department of Mechanical Engineering, NSS College of Engineering

Abstract

The CFD analysis of a rocket engine nozzle has been conducted to understand the phenomena of supersonic flow through it at various divergent angles. A two-dimensional axi-symmetric model is used for the analysis and the governing equations were solved using the finite-volume method in ANSYS FLUENT[®] software. The inlet boundary conditions were specified according to the available experimental information. The variations in the parameters like the Mach number, static pressure, turbulent intensity are being analyzed. The phenomena of oblique shock are visualized and the travel of shock with divergence angle is visualized and it was found that at 15° the shock is completely eliminated from the nozzle. Also the Mach number is found have an increasing trend with increase in divergent angle thereby obtaining an optimal divergent angle which would eliminate the instabilities due to the shock and satisfy the thrust requirements for the rocket.

Keywords - Mach number, oblique shock, finite-volume, turbulent kinetic energy, turbulent dissipation

Date Of Submission: 16, February, 2013



Date Of Publication: 28, February 2013

I. Introduction

Computational Fluid Dynamics (CFD) is an engineering tool that assists experimentation. Its scope is not limited to fluid dynamics; CFD could be applied to any process which involves transport phenomena with it. To solve an engineering problem we can make use of various methods like the analytical method, experimental methods using prototypes. The analytical method is very complicated and difficult. The experimental methods are very costly. If any errors in the design were detected during the prototype testing, another prototype is to be made clarifying all the errors and again tested. This is a time-consuming as well as a cost-consuming process. The introduction of Computational Fluid Dynamics has overcome this difficulty as well as revolutionised the field of engineering. In CFD a problem is simulated in software and the transport equations associated with the problem is mathematically solved with computer assistance. Thus we would be able to predict the results of a problem before experimentation. The current work aims at determining an optimum divergent angle for the nozzle which would give the maximum outlet velocity and meet the thrust requirements. Flow instabilities might be created inside the nozzle due to the formation of shocks which reduce the exit mach number as well as thrust of the engine. This could be eliminated by varying the divergent angle. Here analysis has been conducted on nozzles with divergent angles 4°, 7°, 10°, 13°, 15°. Experimentation using the prototypes of each divergent angle is a costly as well as a time consuming process. CFD proves to be an efficient tool to overcome these limitations. Here in this work the trend of various flow parameters are also analysed.

II. The Mathematical Model

The mathematical model selected for this work is the standard K-ε model which is one of the Reynolds Averaged Navier-Stokes (RANS) model available in fluent. The standard K-ε model is the most widely used transport model. The standard K-ε model is a two-equation model and the two model equations are as follows:

The model equation for the turbulent kinetic energy K is:

$$\frac{DK}{Dt} = \frac{\partial K}{\partial t} + \bar{u}_j \frac{\partial K}{\partial x_j} = \frac{\partial}{\partial x_j} \left[\frac{V_t}{\sigma_k} \frac{\partial K}{\partial x_j} \right] + P - \varepsilon \quad (1)$$

= Rate of increase of K + Convective transport = diffusive transport + Rate of production - Rate of destruction

The model equation for the turbulent dissipation ε is:

$$\frac{D\varepsilon}{Dt} = \frac{\partial\varepsilon}{\partial t} + \bar{u}_j \frac{\partial\varepsilon}{\partial x_j} = \frac{\partial}{\partial x_j} \left[\frac{V_t}{\sigma_\varepsilon} \frac{\partial\varepsilon}{\partial x_j} \right] + C_{\varepsilon 1} \frac{P\varepsilon}{K} - C_{\varepsilon 2} \frac{\varepsilon^2}{K} \quad (2)$$

=Rate of increase of ε + Convective transport= diffusive transport + Rate of production-Rate of destruction

The standard values of all the model constants as fitted with benchmark experiments are (Launder and Sharma, Letters in Heat and mass transport, 1974, 131-138):

$$C_\mu = 0.09 ; \sigma_k = 1.00 ; \sigma_\varepsilon = 1.30 ; C_{\varepsilon 1} = 1.44 ; C_{\varepsilon 2} = 1.92$$

Now the Reynolds stresses are found out using:

$$-\rho \overline{u'_i u'_j} = \frac{2\rho}{3} K \delta_{ij} + \mu_t \left(\frac{\partial \bar{u}_i}{\partial x_j} + \frac{\partial \bar{u}_j}{\partial x_i} \right) \quad (3)$$

And the eddy-viscosity is evaluated as:

$$\mu_t = \rho C_\mu \frac{K^2}{\varepsilon} \quad (4)$$

The major advantages of this model are that it is relatively simple to implement, it leads to stable calculations, and it is a widely validated turbulence model. The known limitation of this model is that its performance is very poor for flows with strong separation, large streamline curvature and high swirling components. Despite of all these limitations, the model is widely accepted model for initial level screening of alternate designs in compressible flows, combustion engineering etc.

2.1 Analysis Procedure

The analysis was run on ANSYS FLUENT[®] software. The geometry of the nozzle was created using the Geometry workbench of ANSYS. A two-dimensional geometry of the nozzle was created. The dimensions and the inlet boundary conditions of the nozzle were obtained from [1] and are as shown in the Table 2.1 below:

Table I: Nozzle dimensions and boundary conditions

Inlet width(m)	1.000
Throat width (m)	0.304
Exit width(m)	0.861
Throat radius of curvature(m)	0.228
Convergent length(m)	0.640
Convergent angle(°)	30
Divergent angle(°)	15
Total pressure(bar)	44.10
Total temperature(K)	3400
Mass flow rate(Kg/s)	826.0

The next task was to mesh the geometry created. The created geometry was imported to the meshing workbench. The mesh used was tetrahedral mesh. The face-mapped meshing option was employed to the geometry in order to avoid the resolution errors. The mesh was refined to the third degree using the refinement option of the workbench. After meshing, the inlet, the axis and the outlet boundaries were named. This meshed geometry is now imported to the FLUENT workbench. In the FLUENT workbench the settings made are as tabulated:

Table II: Problem setup

General	Solver type : Density-based 2D Space: Axi-symmetric
Models	Energy equation : On Viscous model : standard k-ε model
Materials	Air-Ideal gas
Boundary Conditions	Inlet-mass-flow boundary Enter mass flow rate =826kg/s Temperature =3400k Axis-axis boundary Outlet-pressure outlet boundary condition

Table III: Solution

Solution controls	Courant number=0.8
Solution initialization	Compute from : inlet
Run calculation	Check case, Enter number of iterations Click Calculation

The results are obtained when the solution converges. Now we can find the variations in the parameters as follows:

Table IV: Results

Graphics and animation	Use contour option to get the mach number contour, static pressure contour, total temperature contour, turbulent intensity contour
Plots	Use XY plots to plot the mach number Vs position, static pressure Vs position plots

This procedure is continued for various configurations of the nozzle and is compared.

III. RESULTS AND DISCUSSION

3.1 Case1: divergent angle = 4°

3.1Mach number

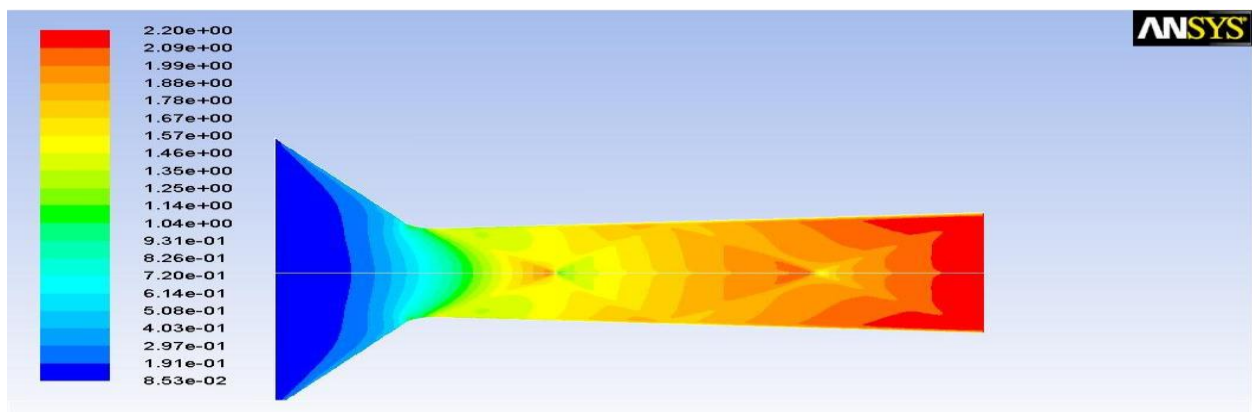


Figure.3.1

The mach contour of the nozzle with the divergent angle of 4° shows the formation of oblique shock in the divergent section. Across the first shock, the Mach number suddenly drops from 2.00 Mach to 1.10 Mach. After this the velocity of flow again increases before the next shock occurs. This shock wave produced is reflected from the walls of the nozzle and it forms another shock in the divergent section itself. At this point, the velocity drops from 2.10Mach to 1.45Mach. It can be seen that the velocity again increases and it reaches 2.20Mach at the exit of the nozzle. The positions where the shock occurs can be determined from the Mach Vs position plot as shown in fig3.2.

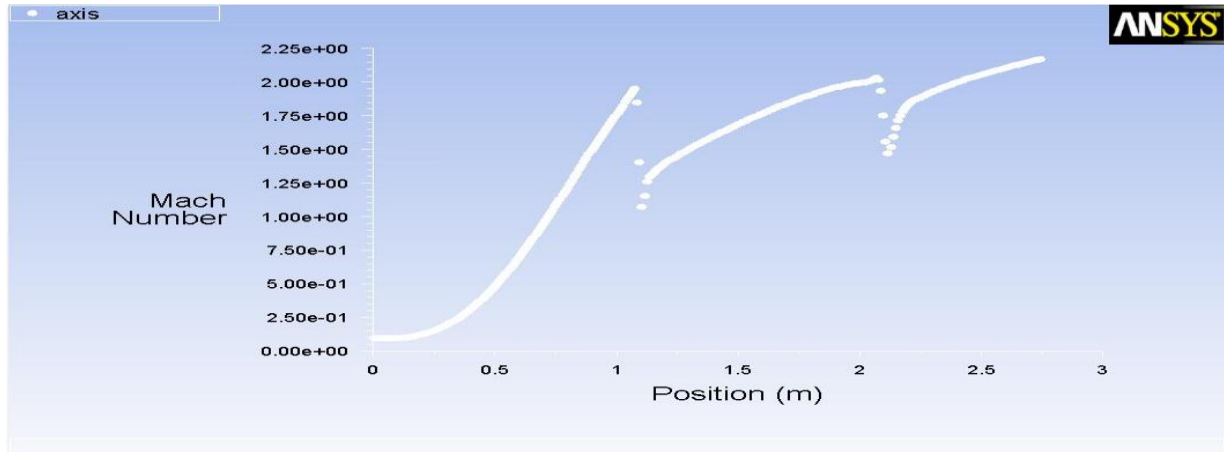


Figure.3.2

It is found that shock occurs at the position 1m from the inlet section and the shock formed due to the reflection of the wave is formed at 2m from the inlet section. The velocity magnitude is found to increase as we move from inlet to exit. The velocity at the inlet is 0.0853Mach (sub-sonic). At the throat section the velocity varies from 0.931Mach to 1.04Mach. The velocity at the exit is found to be 2.2Mach (super-sonic).

3.2 Static pressure

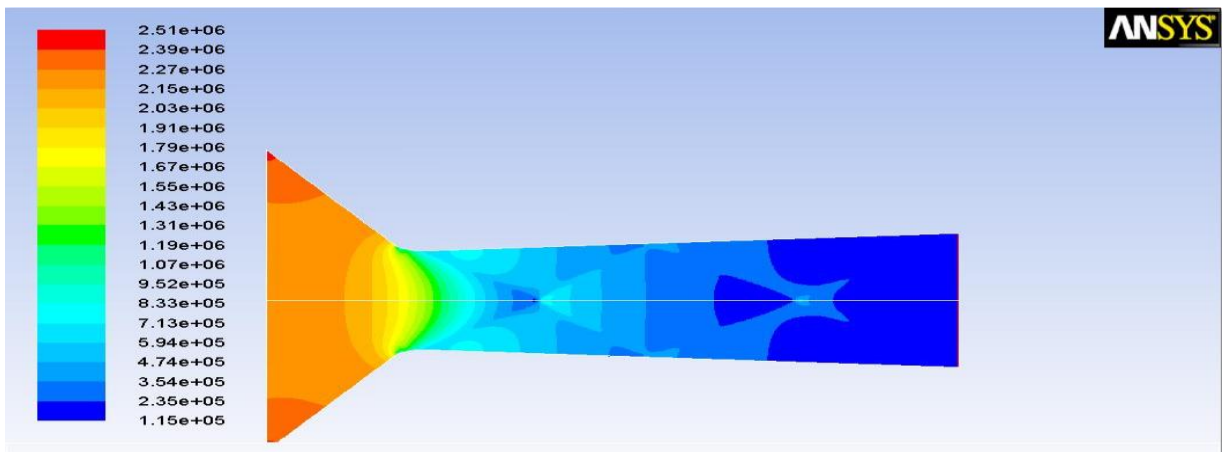


Figure.3.3

Static pressure is the pressure that is exerted by a fluid. Specifically, it is the pressure measured when the fluid is still, or at rest. The above figure reveals the fact that the gas gets expanded in the nozzle exit. The static pressure in the inlet is observed to be 2.39×10^6 Pa and as we move towards the throat there is a decrease and the value at the throat is found out to be 1.67×10^6 Pa. After the throat, there is a sudden increase in the static pressure at the axis which indicates the occurrence of the shock. After the shock there is a slight decrease in the pressure but it again rises at the second shock. Then it reduces to a value of 1.15×10^5 Pa at the exit section due to the expansion of the fluid towards the exit of the nozzle.

3.3 Turbulent intensity

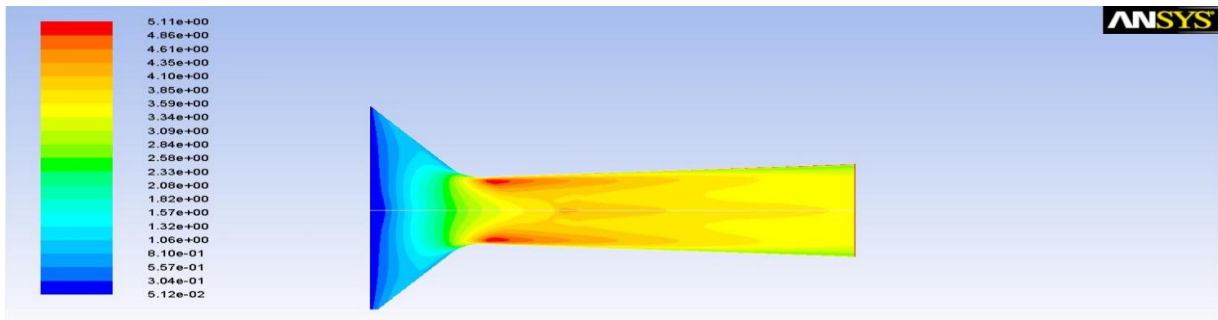


Figure.3.4

The turbulent intensity contour shows that the inlet section has very low turbulence of the value $5.12e-02\%$ and it increases towards the nozzle. Just as the divergent section starts the contour show very high value of turbulent intensity which is due to the sudden expansion of the flow into the divergent section. Here in this case the flow in the divergent section is highly turbulent because of the formation of two shocks inside the section. From the contour the region of first shock has a turbulence intensity of $4.61e+00\%$ and it can be seen that the turbulence prevails even after the second shock. Then it drops to $3.59e+00\%$ at the exit section.

3.2 Case2: divergent angle = 7°

3.2.1 Mach number

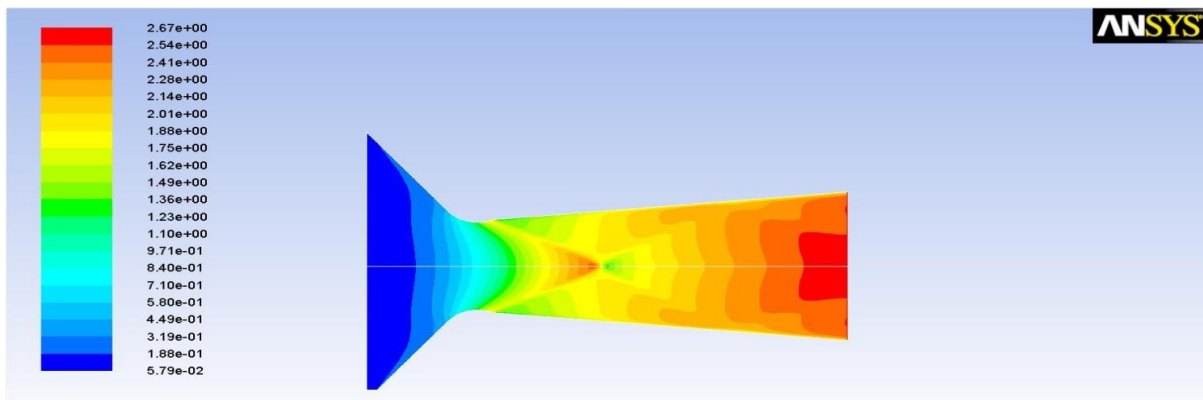


Figure.3.5

The variation in the mach contour with increase in the divergent angle from 4° to 7° can be observed from fig3.5. Here it is noticeable that only one shock has occurred inside the divergent section. The inlet section has a velocity of $5.74e-02$ Mach. At the throat the velocity varies from $9.77e-01$ and 1.11 Mach. Across the shock the velocity drops from 2.5 Mach to 1.5 Mach. The velocity again increases towards the exit of the nozzle. The exit velocity is found to be 2.55 Mach along the axis of the nozzle. The variations in velocity along the walls of the nozzle are due to the viscosity effects.

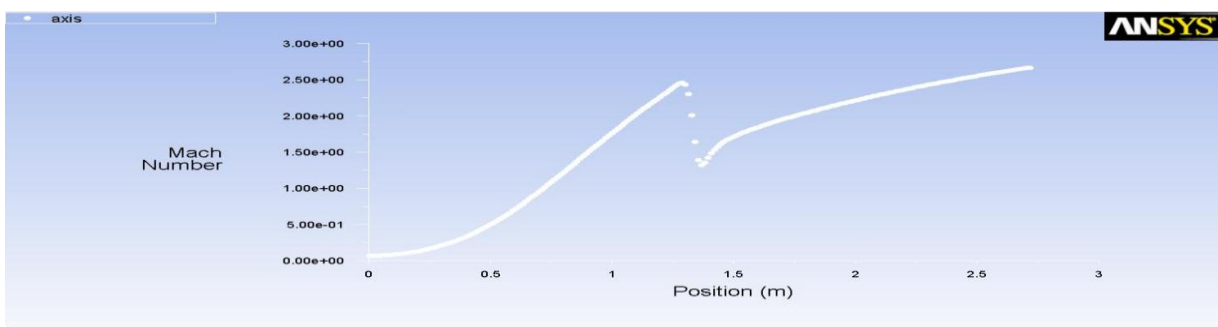


Figure.3.6

The position of shock can be found the mach plot as in fig3.6 and it is observed that the first shock occurs at 1.25m from the inlet. It is thus found that the shock has displaced by about 0.3m as the divergent angle increased from 4° to 7°. The second shock is found to have moved out of the nozzle.

3.4 Static pressure

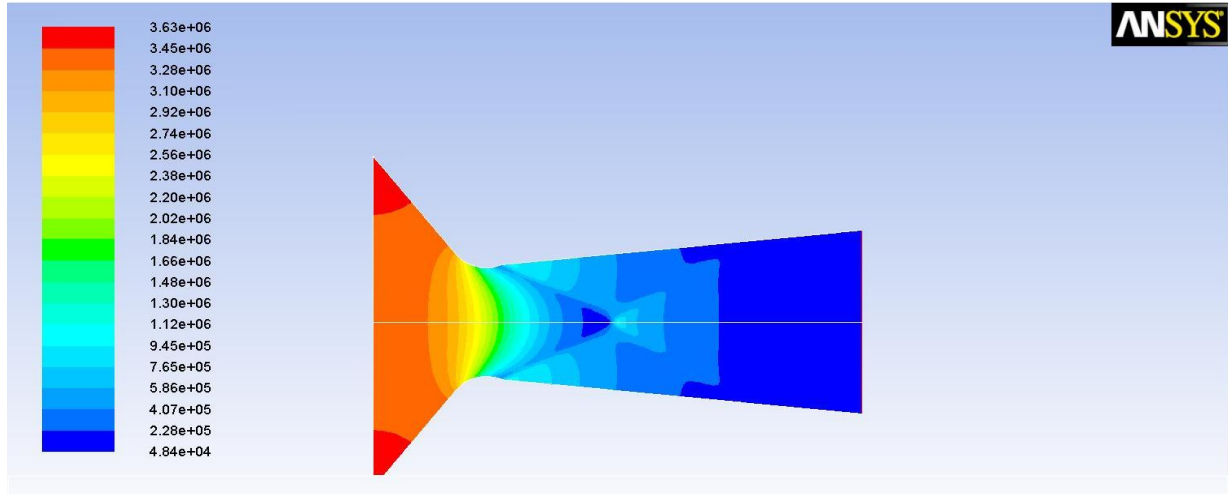


Figure.3.7

The static pressure is found to be 3.46×10^6 Pa at the inlet section. The pressure dropped to about 2.56×10^6 Pa at the throat section and continues to decrease to a value of 4.84×10^4 Pa. At the position of shock it has increased to 1.13×10^6 Pa. Then the static pressure again drops and it reaches a very low value of 4.84×10^4 Pa at the exit section. Compared to the previous case the value of static pressure has dropped.

3.5 Turbulent Intensity

The turbulent intensity contour of the nozzle is as shown in the fig3.8. At the inlet section, it is found that the turbulent intensity is very less, 5.36×10^{-2} %. The turbulent intensity increases as it passes on to the throat section. At the throat section it has reached to a value of 3.63×10^0 %. A sudden increase in the turbulent intensity is seen as the shock initializes. At the initialization of shock it has a value of about 6.61×10^0 % and there occurs a very sudden increase in the turbulence at the shock position. It reaches the maximum value of 1.14×10^1 % at the shock. Then the turbulence decreases, but still the effect of shock has an effect on the turbulence till the exit section. At the exit, the turbulent intensity is about 7.21×10^0 % at the axis.

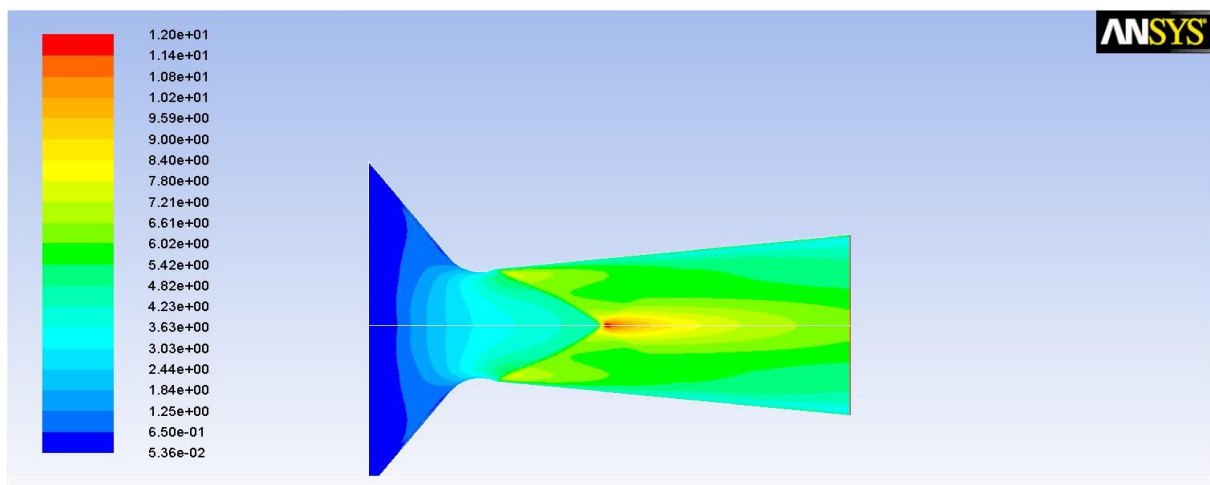


Figure.3.8

3.6 Case3: divergent angle 10°

3.6 Mach number

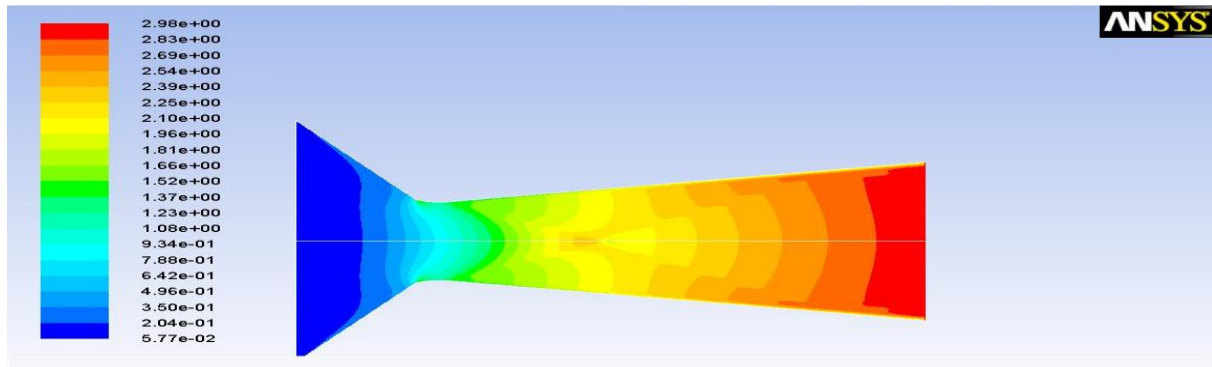


Figure.3.9

The mach contour of the nozzle when the divergent angle is made 10° is shown above. Here also a single oblique shock occurs inside the divergent section. Across the shock, the Mach number is found to drop from 2.50Mach to about 1.75Mach. From the Mach number Vs position plot (fig3.10), it is observed that the shock occurs at about 1.25m from the inlet section. The shock has not much displaced compared to the case when the divergent angle was 7°. But the reduction in Mach number is less compared to the above case. The exit Mach number is 2.98Mach. Another observation is the reduction in flow reversal compared to the 7° case. This can be seen from the mach contour near the walls of the nozzle.

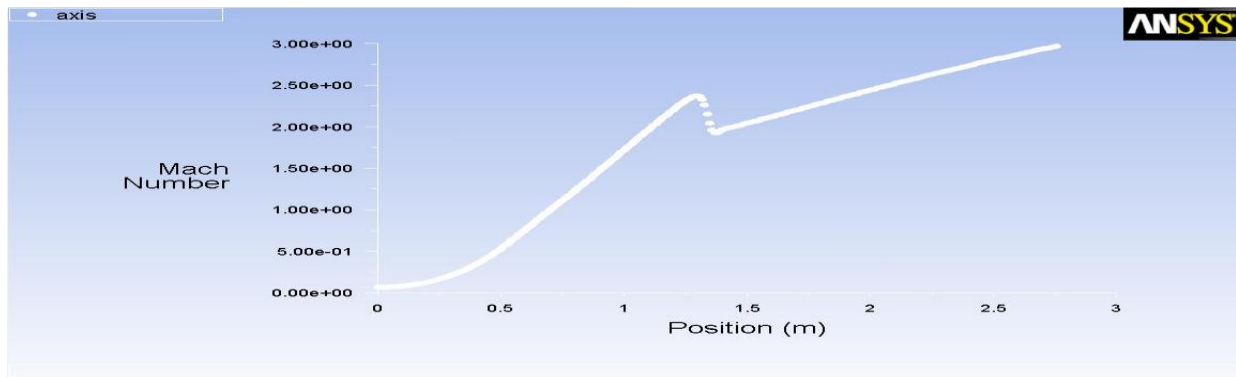


Figure.3.10

3.7 Static pressure

At the inlet section the static pressure is 3.50e+06 Pa and it has dropped to a value of 2.39e+06Pa at the throat section. After the throat section, the static pressure goes on reducing and it drops to a very low value -7.06e+02 Pa at the exit section. An increase in the value of static pressure is seen which represents the shock. The static pressure has dropped considerably compared to the above cases.

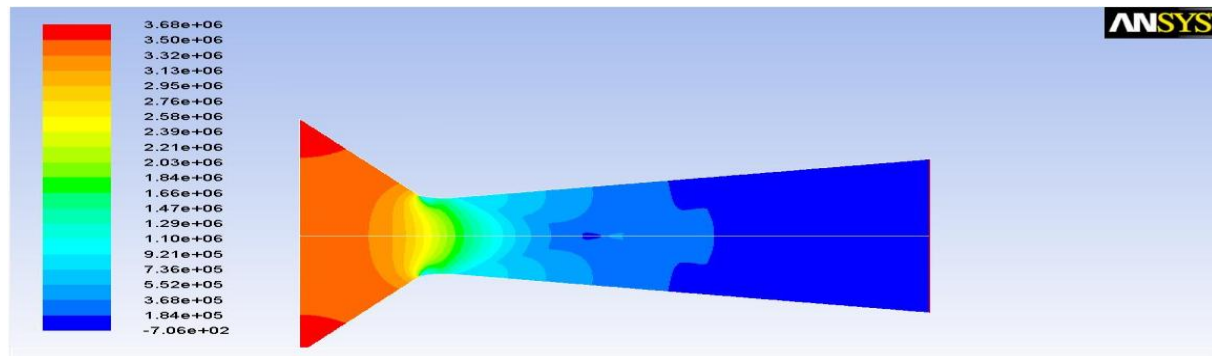


Figure.3.11

3.8 Turbulent Intensity

The turbulent intensity at the inlet section is $5.31e-02\%$ which is a very small value. This value increases towards the throat section and reaches $2.18e+00\%$. The sudden change in cross sectional area has caused an increase in turbulence intensity near the walls. This turbulence gets diffused as the cross sectional area increases further. Most importantly, the turbulence value shows a sudden increase at the position of shock. At the shock it has reached a value of $4.91e+00\%$. A very close observation shows high turbulent intensity near the exit walls. This may be because of the viscosity effects.

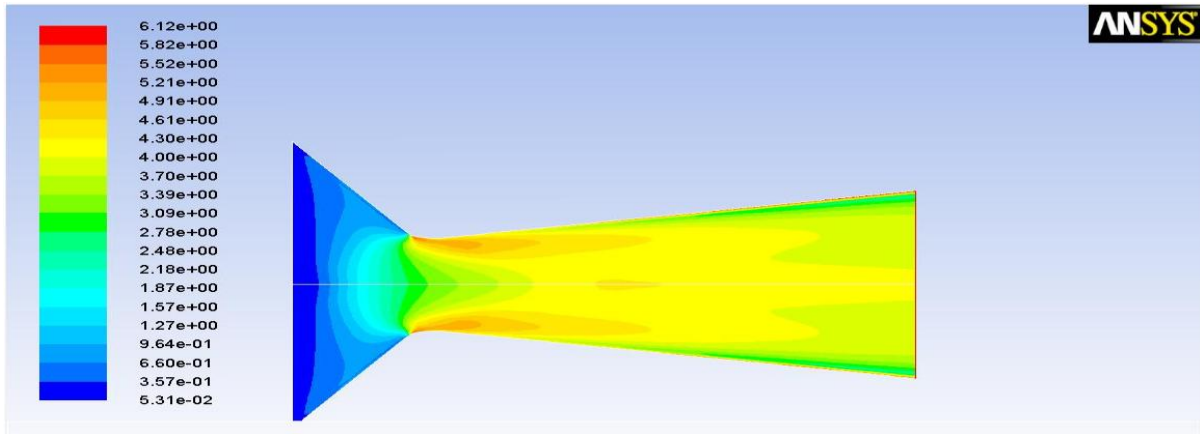


Figure.3.12

3.9 Case4: divergent angle 13°

3.9 Mach number

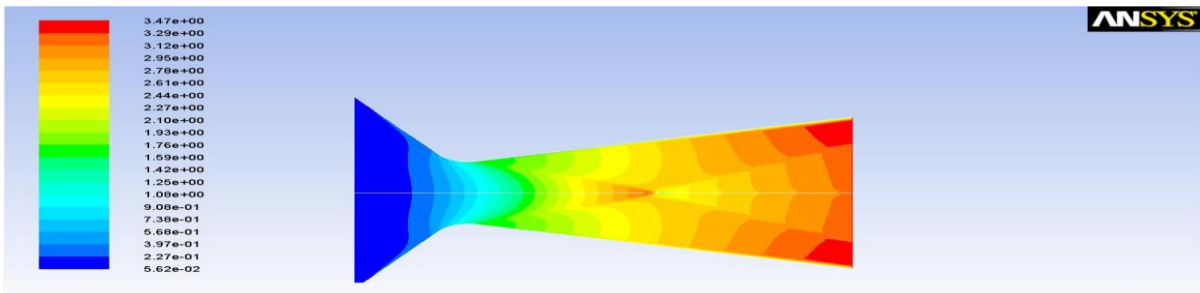


Figure.3.13

The above figure shows the Mach contour of the nozzle when the divergent angle is made 13° . The inlet velocity is $5.62e-02$ Mach. The velocity increases to $9.08e-01$ Mach at the throat. The velocity goes on increasing as it passes through the divergent section and it can be seen that oblique shock has developed in this case also. Across the section, the velocity has dropped from $3.25e+00$ Mach to $2.00e+00$ Mach. The exit velocity is found to be $3.29e+00$ Mach at the axis of the exit section. But the velocity at the exit section near the walls of the nozzle is found to be $3.47e+00$ Mach which is more than then velocity at axis. This is because of the effect of the shock wave travelling towards the exit section.

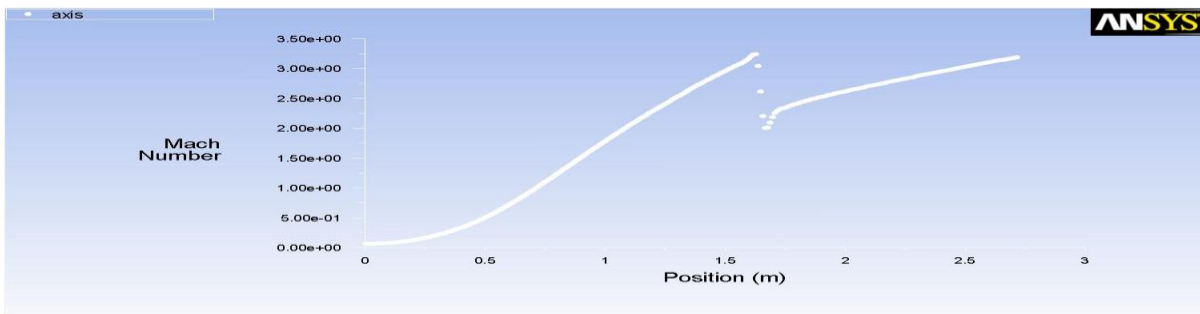


Figure.3.14

The position of shock as found from Mach number Vs Position is 1.6m from the inlet section. It is evident that the position of shock has displaced towards the exit section compared to the previous cases.

3.10 Static pressure

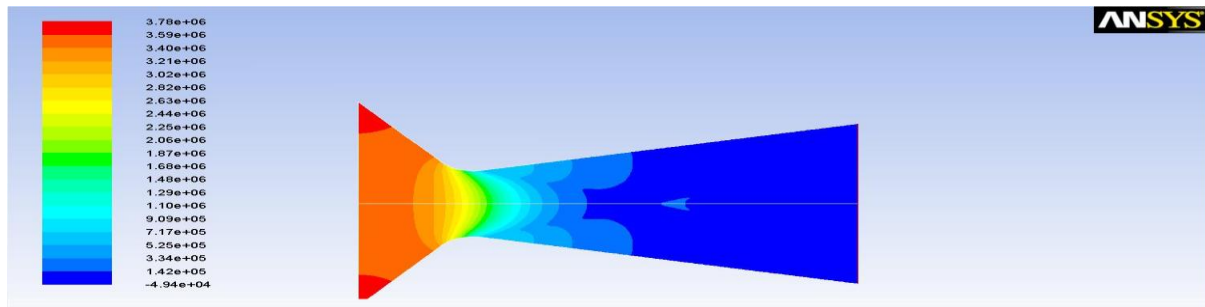


Figure.3.15

The static pressure contour is as shown in fig3.15. The inlet static pressure is $3.40e+06$ Pa and it has reduced towards the throat and has reached a value of $2.63e+06$ Pa at the throat. It has still decreased to a low value of $-4.94e+04$ Pa and has remained almost constant except at the region of shock where a small increase in static pressure is seen.

3.11 Turbulent intensity

At the inlet section the turbulent intensity is found to be $5.32e-02\%$. It has increased to a value of $2.42e+00$ at the throat and keeps on increasing throughout the divergent section. A small increase in the value of turbulent intensity is seen at the portion where the throat transforms to divergent section and also at the region of shock. At shock the turbulent intensity rises to a value of $5.79e+00\%$ and the effect of shock is seen till the exit

section near the axis of the nozzle. A decrease in the turbulent intensity is seen at the walls of the divergent section which could be justified as viscous effects.

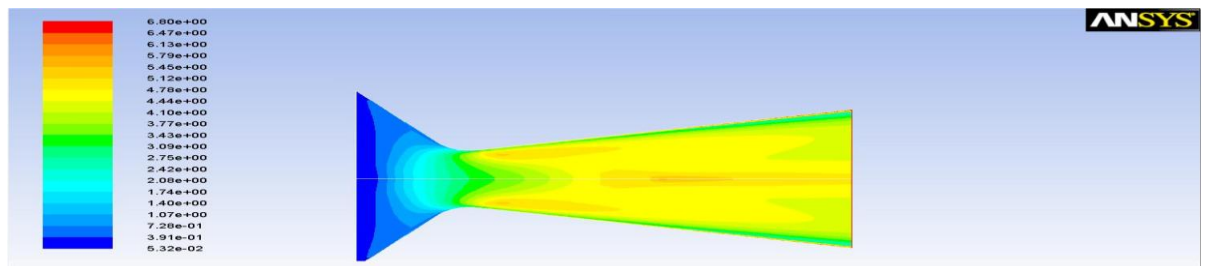


Figure.3.16

3.12 Case5: divergent angle 15°

3.12 Mach number

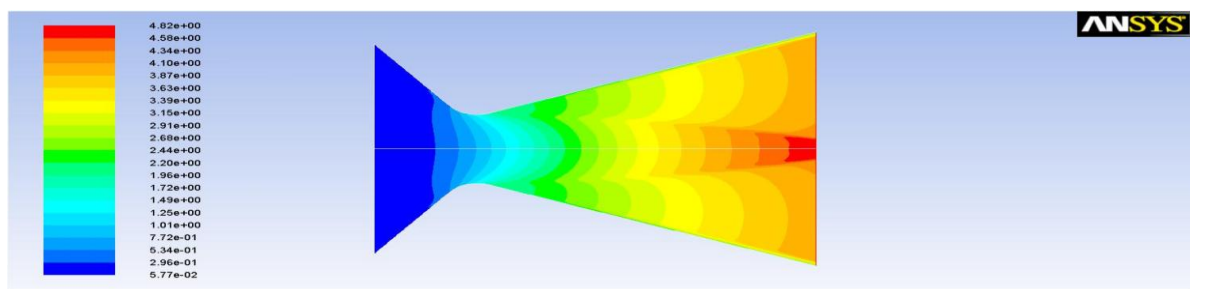


Figure.3.17

The Mach contour of the CD nozzle when the divergent angle is made 15° is shown in the figure. It is clear that the shock has been completely eliminated from the divergent section of the nozzle. The inlet section has a velocity of $5.77e-02$ Mach and it increases to a value of $7.72e-01$ Mach at the throat section. The velocity is found to be increasing as it passes through the divergent section. At the exit section, the velocity is found to be $4.82e+00$ Mach.

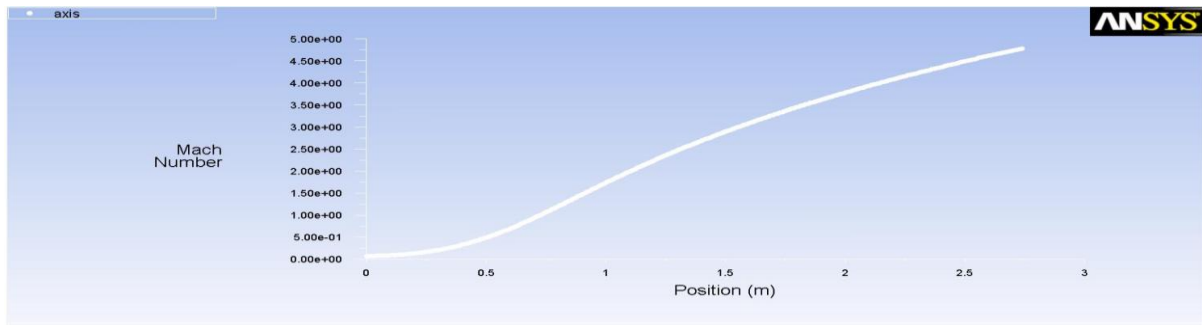


Figure.3.18

The Mach number Vs position plot also shows a continuous increase in the velocity from inlet section to the outlet section. And there is no sudden drop in velocity which shows that no shock is occurring in the nozzle.

3.13 Static Pressure

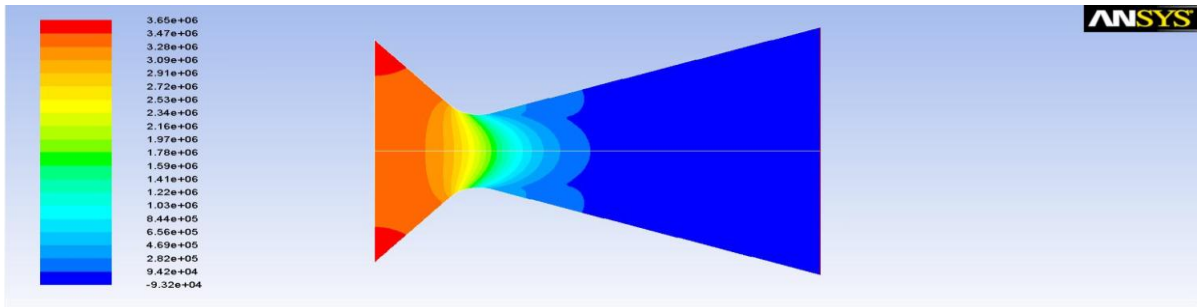


Figure.3.19

The static pressure contour shows a reduction in the static pressure throughout the nozzle. At the inlet, the static pressure is found to be $3.47e+06$ Pa. At the throat it has reduced to $2.53e+06$ Pa. This value again reduces to a value of $-9.32e+04$ Pa and remains constant till the exit section.

3.14 Turbulent intensity

The turbulent intensity contour shows that at the inlet the turbulent intensity is $5.21e-02\%$. It has increased to $2.29e+00\%$ at the throat section. Since the divergent angle is higher, the sudden expansion has caused the turbulence at the beginning of the divergent section. It is also seen that the increasing velocity towards the exit section also has caused a turbulence of flow towards the exit section. The value of turbulence is found to be $6.75e+00\%$ in this region.

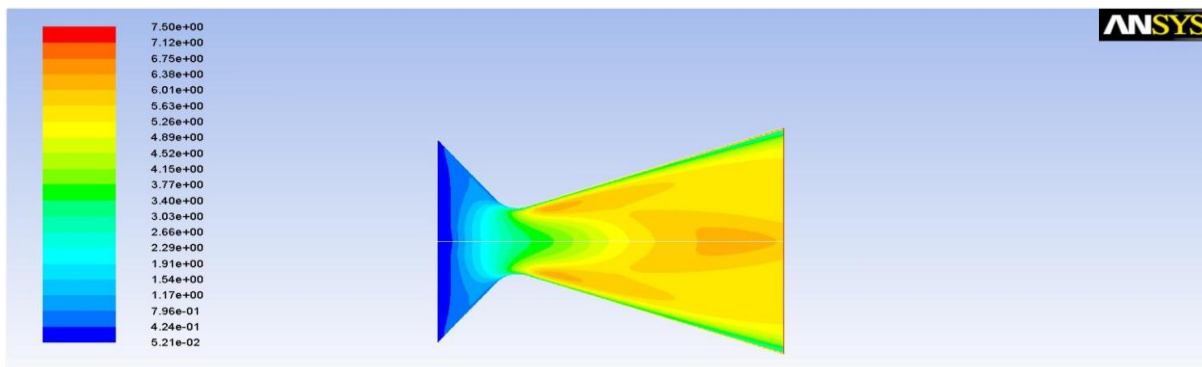


Figure.3.20

IV. Conclusions

Results tables

Table V Conditions at exit section

CASE	ANGLE(deg)	MACH NUMBER	STATIC PRESSURE (Pa)	TURBULENT INTENSITY (%)
1	4	2.20e+00	1.15e+05	3.59e+00
2	7	2.67e+00	4.84e+04	6.61e+00
3	10	2.98e+00	-7.06e+02	4.30e+00
4	13	3.29e+00	-4.94e+04	5.79e+00
5	15	4.82e+00	-9.32e+04	6.01e+00

Table VI Conditions at throat section

CASE	ANGLE(deg)	MACH NUMBER	STATIC PRESSURE(Pa)	TURBULENT INTENSITY(%)
1	4	8.26e-01	1.91e+06	3.09e+00
2	7	9.71e-01	2.74e+06	4.23e+00
3	10	9.34e-01	2.76e+06	3.09e+00
4	13	1.08e+00	2.82e+06	3.97e+00
5	15	1.25e+00	2.72e+06	2.66e+00

- At the exit section, the Mach number is found to increase with increase in divergent angle. It is 2.20e+00Mach for 4° and it increases to the highest value of 4.82e+00Mach for 15°. Similarly at the throat section also, the Mach number goes on increasing with increase in divergent angle. It has increase from 8.26e+01Mach at 4° to 1.25e+00Mach at 15°.
- The static pressure decreases with increased divergent angle. At 4° it was 1.91e+06Pa and it decreased to a value of -9.32e+004Pa.
- It was observed that oblique shocks are formed during flow through the nozzle. When the divergent angle was 4°, the first shock occurred at 1m from the inlet and this wave reflected from the walls of the nozzle has caused another shock at 2m. It was found that the increase in divergent angle displaces the shock towards the exit of the nozzle. When the divergent angle was made 7° the shock was formed at 1.25m from inlet and the second shock is eliminated from the nozzle. As we further increase the angle to 13°, the shock is formed at 1.6m from inlet. As we increase it to 15°, it is observed that the shock is completely eliminated from the nozzle and this could be considered as a good design for the nozzle. The trends are similar to referred works as in [2] and [3].
- As a verification of the results obtained, a prototype of the 15° nozzle can be made and flow visualisation techniques such as schlieren photographic technique could be used for verification of the flow patterns.

VII. ACKNOWLEDGEMENT

The authors would like to acknowledge late Prof. C K Anilkumar, former Head of Department, Mechanical Engineering, NSS College of Engineering, who always had been a source of inspiration and ignited the fire of research in the hearts of authors.

Reference

- [1] Varun, R.; Sundararajan,T.; Usha,R.; Srinivasan,k.; Interaction between particle-laden under expanded twin supersonic jets, Proceedings of the Institution of Mechanical Engineers, Part G: Journal of Aerospace Engineering 2010 224: 1005.
- [2] Pandey,K.M.; Singh, A.P.; CFD Analysis of Conical Nozzle for Mach 3 at Various Angles of Divergence with Fluent Software, International Journal of Chemical Engineering and Applications, Vol. 1, No. 2, August 2010, ISSN: 2010-0221.
- [3] Natta, Pardhasaradhi.; Kumar, V.Ranjith.; Rao, Dr. Y.V. Hanumantha.; Flow Analysis of Rocket Nozzle Using Computational Fluid Dynamics (Cfd), International Journal of Engineering Research and Applications (IJERA), ISSN: 2248-9622,Vol. 2, Issue 5, September- October 2012, pp.1226-1235.
- [4] K.M. Pandey, Member IACSIT and A.P. Singh. K.M.Pandey, Member, IACSIT and S.K.YadavK.M.Pandey and S.K.Yadav, —CFD Analysis of a Rocket Nozzle with Two Inlets at Mach2.1, Journal of Environmental Research and Development, Vol 5, No 2, 2010, pp- 308-321.
- [5] Shigeru Aso, ArifNur Hakim, Shingo Miyamoto, Kei Inoue and Yasuhiro Tani “ Fundamental study of supersonic combustion in pure air flow with use of shock tunnel” Department of Aeronautics and Astronautics, Kyushu University, Japan , Acta Astronautica 57 (2005) 384 – 389.
- [6] P. Padmanathan, Dr. S. Vaidyanathan, Computational Analysis of Shockwave in Convergent Divergent Nozzle, International Journal of Engineering Research and Applications (IJERA), ISSN: 2248-9622 , Vol. 2, Issue 2,Mar-Apr 2012, pp.1597-1605.
- [7] Adamson, T.C., Jr., and Nicholls., J.A., “On the structure of jets from Highly under expanded Nozzles into Still Air,” Journal of the Aerospace Sciences, Vol.26, No.1, Jan 1959, pp. 16-24.
- [8] Lewis, C. H., Jr., and Carlson, D. J., “Normal Shock Location in under expanded Gas and Gas particle Jets,” AIAA Journal, Vol 2, No.4, April 1964, pp. 776-777.

Books

- [9] Anderson, John D.Jr.; Modern Compressible Flow with Historical Perspective, Third edition, 2012
- [10] Versteeg. H.; Malalasekra.W.; An Introduction to Computational Fluid Dynamics The Finite Volume Method, Second Edition,2009

Biographies And Photographs

The first author is currently a student of Department of Mechanical Engineering, NSS College of Engineering, Kerala, India. Author is enthusiastic in the field of Propulsion and also fluid mechanics. The second author is a post-graduate in Aerospace Engineering from IIT madras, Chennai, India. Author is currently working as an assistant professor in the Department of Mechanical Engineering, NSS College of Engineering, Kerala, India. He is an expert in the field of fluid mechanics and aerodynamics.